Bioorganic & Medicinal Chemistry Letters 29 (2019) 1874–1880

Contents lists available at ScienceDirect

Bioorganic & Medicinal Chemistry Letters

journal homepage: www.elsevier.com/locate/bmcl

Development of substituted pyrido[3,2-*d*]pyrimidines as potent and selective dihydrofolate reductase inhibitors for pneumocystis pneumonia infection

Khushbu Shah[a], Sherry Queener[b], Vivian Cody[c], Jim Pace[c], Aleem Gangjee[a]

[a] Division of Medicinal Chemistry, Graduate School of Pharmaceutical Sciences, Duquesne University, Pittsburgh PA 15282, United States
[b] Department of Pharmacology and Toxicology, Indiana University School of Medicine, Indianapolis, IN 46202, United States
[c] Hauptman-Woodward Medical Research Institute, 700 Ellicott Street, Buffalo, NY 14203, United States

ARTICLE INFO

Keywords:
PCP
DHFR
Pyrido[3,2-*d*]pyrimidines
Pneumocystis jirovecii

ABSTRACT

Pneumocystis pneumonia (PCP) caused by *Pneumocystis jirovecii* (pj) can lead to serious health consequences in patients with an immunocompromised system. Trimethoprim (TMP), used as first-line therapy in combination with sulfamethoxazole, is a selective but only moderately potent pj dihydrofolate reductase (pjDHFR) inhibitor, whereas non-clinical pjDHFR inhibitors, such as, piritrexim and trimetrexate are potent but non-selective pjDHFR inhibitors. To meet the clinical needs for a potent and selective pjDHFR inhibitor for PCP treatment, fourteen 6-substituted pyrido[3,2-*d*]pyrimidines were developed. Comparison of the amino acid residues in the active site of pjDHFR and human DHFR (hDHFR) revealed prominent amino acid differences which could be exploited to structurally design potent and selective pjDHFR inhibitors. Molecular modeling followed by enzyme assays of the compounds revealed **15** as the best compound of the series with an IC_{50} of 80 nM and 28-fold selectivity for inhibiting pjDHFR over hDHFR. Compound **15** serves as the lead analog for further structural variations to afford more potent and selective pjDHFR inhibitors.

Introduction

Pneumocystis carinii pneumonia (PCP) caused by *Pneumocystis jirovecii* is a fungal infection which affects patients with altered host immunity, such as, patients with cancer, transplant recipients, patients with HIV/AIDS and patients on immunosuppressive medications. [1–6] In HIV patients, PCP leads to pulmonary inflammation, hospitalization, and death.[7–10] If left untreated, PCP is almost always fatal. Even when treated, the mortality rate is 10%.[11] In the USA, 9% of HIV infected patients and 1% of organ transplant recipients develop PCP infection.[12] Although PCP prophylaxis and highly active antiretroviral therapy (HAART) in AIDS has decreased the incidences of PCP infection, cases still persist due to non-adherence to HIV medication, toxicity to the HIV medications, emergence of drug resistant HIV strains, late diagnosis of HIV and the rise of the number of HIV cases in developing countries along with resistance to currently used drugs for PCP.[13,14]

For past few decades, oral administration of trimethoprim (TMP)-sulfamethoxazole (SMX) combination (co-trimoxazole) has been the first line choice for both prophylaxis and treatment of PCP.[15,16] The combination synergistically blocks folic acid synthesis, since TMP (Fig. 1) is a selective, but weak inhibitor of dihydrofolate reductase (DHFR)[17], while SMX is an inhibitor of dihydropteroate synthase (DHPS).[18] The low activity of TMP against DHFR is augmented by SMX in the treatment regimen. This combination is less well tolerated in patients with HIV/AIDS, where 50–80% experience side-effects due to SMX. The most common one being a diffuse maculopapular rash, sometimes accompanied with fever which often leads to discontinuation of treatment.[19,20] The alternative therapy can be (i) pentamidine (intravenous – infused over an hour); (ii) TMP-dapsone (oral); or (iii) clindamycin (intravenous) – primaquine (oral), which are not preferred due to higher prevalence of side-effects and in some cases lower efficacy.[15,21–24] Experimental drugs such as piritrexim (PTX) and trimetrexate (TMQ) (Fig. 1) are potent, but non-selective inhibitors of DHFR, which cause dose-limiting toxicities.[15,25,26] Thus, for patients who do not respond to first line treatment, development of effective and safe drugs for the treatment of PCP is critically warranted. Our long-term goal is to provide analogs with excellent potency along with high selectivity for *Pneumocystis jirovecii* DHFR (pjDHFR) over human DHFR

Abbreviations: DHPS, dihydropteroate synthase; PCP, Pneumocystis carinii pneumonia; hDHFR, human dihydrofolate reductase; pcDHFR, *Pneumocystis carinii* dihydrofolate reductase; pjDHFR, *Pneumocystis jirovecii* dihydrofolate reductase; PTX, Piritrexim; TMP, Trimethoprim; TMQ, Trimetrexate; SMX, Sulfamethoxazole

E-mail address: gangjee@duq.edu (A. Gangjee).

https://doi.org/10.1016/j.bmcl.2019.06.004
Received 12 May 2019; Received in revised form 28 May 2019; Accepted 1 June 2019
Available online 04 June 2019
0960-894X/

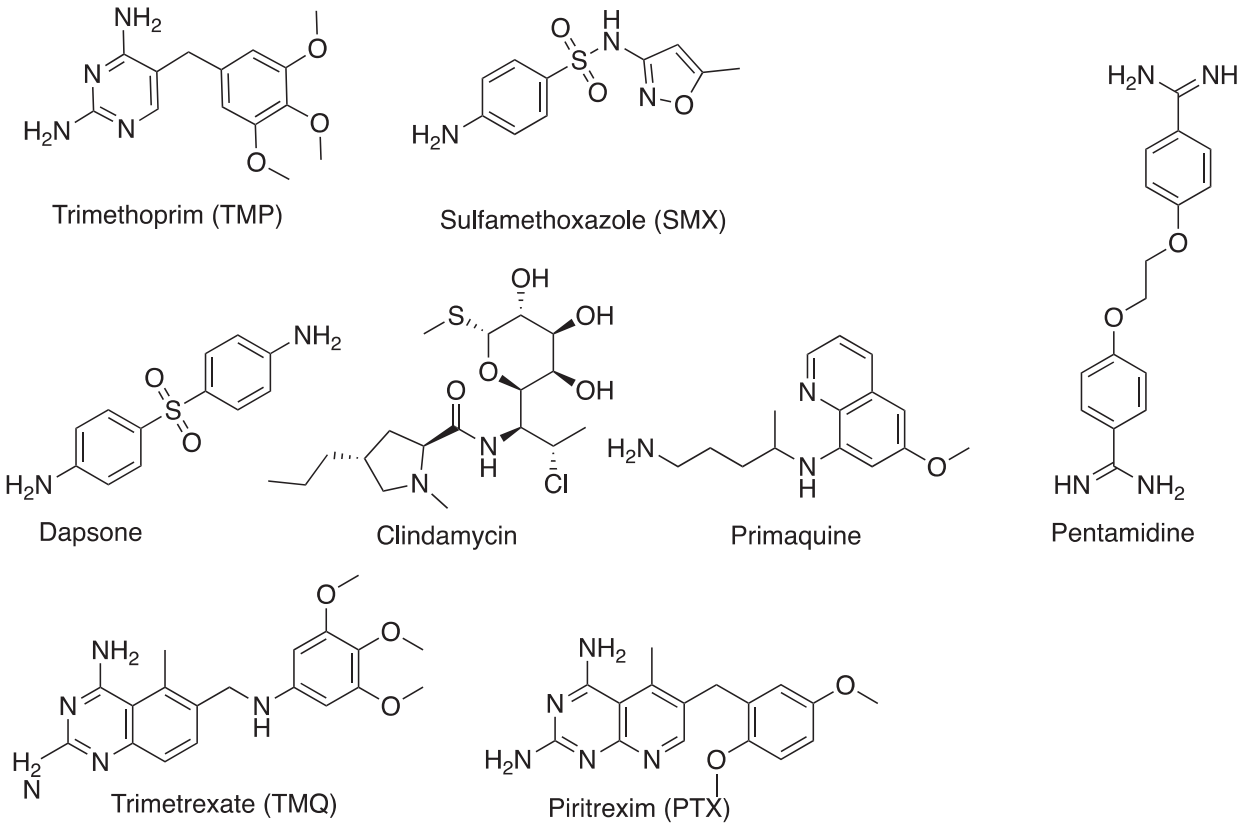

Figure 1. Agents that have been used to treat PCP.

(hDHFR). Such agents could be used alone as well as in combination with sulfonamides and other drugs for PCP infections in humans.

Although it has been widely known that PCP is a host specific infection, drugs designed for PCP have been evaluated against *Pneumocystis carinii* DHFR (pcDHFR), and not pjDHFR.[17,27] *Pneumocystis carinii (pc)*, the causative species in rats is different from *Pneumocystis jirovecii* responsible for human infections. There is a 38% difference in the amino acid sequence of pcDHFR and pjDHFR which suggests that drugs evaluated against the surrogate pcDHFR *in vitro* or *in vivo*, may not translate to the treatment of PCP infection in humans.[28,29] In the absence of crystal structure information for pjDHFR, a tissue culture or a PCP animal model for *in vitro* studies for PCP cause severe impediments in drug discovery efforts. In fact, since the preliminary evaluation of TMP/SMX there has been no new treatment for PCP caused by *P. jirovecii* that could effectively supplant TMP/SMX.

Gangjee and coworkers[28] reported pyrido[2,3-*d*]pyrimidines **1–6** as somewhat selective and potent pjDHFR inhibitors (Table 1).

To compare the binding of **1** in the active sites of pjDHFR and hDHFR, a docking study of **1** was performed using the refined reported homology model of pjDHFR [32] and the crystal structure of hDHFR in Schrödinger.[31] In pjDHFR, the pyrido[2,3-*d*]pyrimidine scaffold is stabilized by a π-π stacking interaction with Phe36. The protonated N1 and 2-NH_2 of **1** form an ionic bond with Asp32 in the form of a salt bridge. The 4-NH_2 forms hydrogen bonding interaction with the backbone carbonyl of Ile10. The side chain phenyl ring is oriented in a pocket formed by Leu25, Met33, Ser64, and Leu65. The N^9-H group is oriented towards the Ile123 side chain. In hDHFR, the pyrido[2,3-*d*] pyrimidine scaffold is also stabilized by a π-π stacking interaction with Phe34. The protonated N1 and 2-NH_2 form an ionic bond with Glu30. The 4-NH_2 forms hydrogen bonding interaction between the backbone carbonyl of Ile7. The side chain phenyl ring is oriented in a pocket formed by Leu22, Phe31, Ser59, and Ile60. The N^9-H group is oriented towards the Val115 side chain. The docking scores of **1** in the pjDHFR homology model and hDHFR crystal structure were −7.88 kcal/mol and −9.54 kcal/mol, respectively. The in vitro IC_{50} values of **1** reflect the docking scores obtained with the inhibition of hDHFR somewhat better than that for pjDHFR for **1** (Table 1). This provides validation of our docking protocol in the homology model of pjDHFR compared with docking in hDHFR crystal structure.

The amino acids that constitute the active site of pjDHFR and hDHFR, as visible from Fig. 2, are quite distinct. The hDHFR active site contains Phe31, Ile60, and Val115, whereas active site of pjDHFR contains Met33, Leu65, and Ile123. The different amino acids

Table 1
Inhibitory Concentrations (IC_{50}, in nM) against Recombinant DHFR from pjDHFR and human DHFR (hDHFR) and Selectivity Ratios[28].

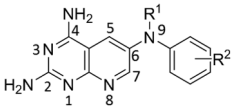

	R^1	R^2	pjDHFR (IC_{50}, in nM)	hDHFR (IC_{50}, in nM)	Selectivity Ratio [hDHFR/pjDHFR]
1	H	H	300	190	< 1
2	H	4-CH_3	620	2100	3
3	H	4-OCH_3	400	3650	9
4	H	2′,3′-$(CH)_4$	250	2100	8
5	H	3′,4′-$(CH)_4$	400	2200	5
6	H	3′,4′,5′-triF	870	3100	4
TMP			120	32,200	268
PTX			1.6	3.0	2
TMQ			2.1	2.6	1

These assays were carried out at 37 °C under 18 μM dihydrofolic acid concentration. The standard error of the means for these values is 12% or less than the mean value; [b]Trimethoprim; [c]Piritrexim.

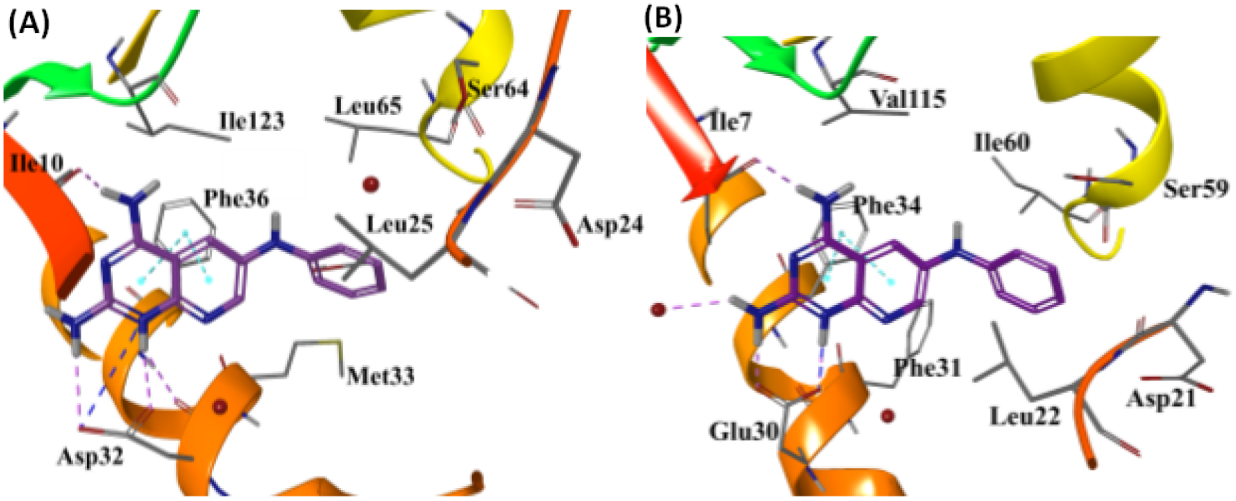

Figure 2. (A) Docked pose of **1** (magenta) in the homology model of pjDHFR and (B) Docked pose of **1** (magenta) in the crystal structure of hDHFR (PDB: 4QJC, 1.62 Å)[30]

occupying the same location in the active sites, such as Met33 (in pjDHFR) vs. Phe31 (in hDHFR) and Ile 123 (in pjDHFR) vs. Val115 (in hDHFR), possess varied shapes, sizes and electronic properties. Such differences can be exploited for the design of inhibitors to provide potency and selectivity for pjDHFR over hDHFR. We reported our efforts in targeting the amino acid difference of Met33 (in pjDHFR) and Phe31 (in hDHFR) by varying substitutions on the 7-position of a truncated pyrrolo[2,3-*d*]pyrimidine scaffold.[32] The 6-subtituted pyridopyrimidines evaluated thus far against pjDHFR consist of the pyrido [2,3-*d*]pyrmidine scaffold. No study of significant variation of the scaffold has been carried out to our knowledge.

Gangjee *et al.*[34] reported the pyrido[2,3-*d*]pyrimidines and their analogs as inhibitors of pcDHFR. Rosowsky *et al.*[33] synthesized and evaluated the regioisomeric pyrido[3,2-*d*]pyrimidine analogs as inhibitors of pcDHFR. The biological evaluation of pyrido[3,2-*d*]pyrimidine **7** (Table 2) in pcDHFR and rat liver DHFR (rlDHFR) displayed a 5-fold increase in potency for pcDHFR, compared to its regio pyrido [2,3-*d*]pyrimidine analog **8** (Table 2). This comparison suggested that scaffold replacement of a pyrido[2,3-*d*]pyrimidine to a pyrido[3,2-*d*] pyrimidine improved the potency for pcDHFR and a similar approach could perhaps be useful to improve the potency for pjDHFR. Gangjee at al. [33] also reported 6-substituted pyrido[3,2-*d*]pyrimidines as inhibitors of pcDHFR. However because of the amino acid differences, as reported in Shah et al.,[31] it has been validated that activity against pcDHFR does not translate into activity against pjDHFR. Hence, it was important to synthesize and evaluate the pyrido[3,2-*d*]pyrimidine series of compounds as selective pjDHFR inhibitors, (Fig. 3).

To study the probable binding modes of compounds obtained via a scaffold hopping of pyrido[2,3-*d*]pyrimidine with pyrido[3,2-*d*]pyrimidine, **9** (Fig. 3) was docked in the active sites of pjDHFR and hDHFR using the reported homology model of pjDHFR and crystal structure of hDHFR, with Schrödinger.[28,30] (Fig. 4). The pyrido[3,2-*d*]pyrimidine **9** exhibited a similar docked pose as **1** suggesting the scaffold binding could be at least as favorable as the pyrido[2,3-*d*]pyrimidine scaffold. The docking scores of **9** in the pjDHFR homology model and hDHFR crystal structure were − 8.22 kcal/mol and − 8.87 kcal/mol, respectively. Compared to the docking score of **1** in the pjDHFR homology model (-7.88 kcal/mol), **9** displayed a higher binding potential to pjDHFR, whereas compared to the docking score of **1** in hDHFR crystal structure (-9.54 kcal/mol), **9** displayed a lower binding potential to hDHFR. This suggested that a scaffold change from pyrido[2,3-*d*]pyrimidine to pyrido[3,2-*d*]pyrimidine could afford increased potency and selectivity for pjDHFR.

The reported pyrido[2,3-*d*]pyrimidine compounds **1–6** (Table 1) displayed moderate potencies for pjDHFR, but none were significantly selective for pjDHFR over hDHFR. Compounds **9–17** (Fig. 3), were designed as pyrido[3,2-*d*]pyrimidine analogs of **1–6**. The shape of the pjDHFR active site and hDHFR active site differ due to presence of Met33 (flexible residue) and Leu65 in pjDHFR and Phe31 (bulkier residue) and Ile60 in hDHFR. Compounds **9–12** (Fig. 3) were designed as analogs of **1–3** (Table 1) to determine the influence of the pyrido[3,2-*d*] pyrimidine system and the electron donating substitutions on the side chain aryl group on activity against pjDHFR and hDHFR. These compounds were anticipated to provide a structure activity relationship through electron donating groups (inductive and resonance). Compounds **13** and **14** (Table 3) were designed as pyrido[3,2-*d*]pyrimidine analogs of **4** and **5** (Table 1). Due to the bulkier size of the naphthyl group, the side chains of these proposed compounds were expected to sterically clash with the side chain Phe31 in hDHFR. This clash is absent in pjDHFR, since the pjDHFR active site is composed of a flexible Met33 residue instead of Phe31 (in hDHFR) at this position. Compounds **15–17** (Table 3) were designed as analogs of **6** (Table 1). These compounds contain electron withdrawing groups to evaluate their influence on DHFR inhibitory activity.

As observed from the docking of **9** and **18** in Fig. 5, the *N*-CH_3 of **18** is oriented towards the Ile123 side chain in the pjDHFR active site. An appropriate alkyl substitution on the nitrogen lead to compounds that can interact with the longer Ile123 (in pjDHFR) and not with shorter Val115 (in hDHFR). Hence, the *N*-CH_3 analog **18** would be expected to afford an improvement in pjDHFR potency and selectivity over hDHFR. Docking of **18** in the active site of pjDHFR using the reported homology model of pjDHFR and superimposition of the docked pose of **18** in the active site of pjDHFR over the docked pose of **9** in the active site of pjDHFR is shown in Fig. 5a. The docking study revealed that both compounds display a bidentate ionic bond between the protonated N1

Table 2
Inhibition Concentrations (IC_{50}) against pcDHFR and rlDHFR [33, 34].

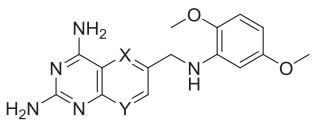

#	X	Y	pcDHFR (nM)	rlDHFR (nM)
7	N	C	1400	430
8	C	N	6100	500

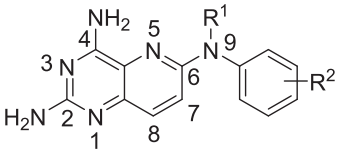

	R^1	R^2
9	H	H
10	H	4'-CH_3
11	H	4'-OCH_3
12	H	4'-OH
13	H	2',3'-$(CH)_4$
14	H	3',4'-$(CH)_4$
15	H	3',4'-diF
16	H	3',4',5'-triF
17	H	4'-OCF_3
18	CH_3	H
19	CH_2CH_3	H
20	$CH_2CH_2CH_3$	H
21	$CH(CH_3)_2$	H
22	$CH_2CH_2CH_2CH_3$	H

Figure 3. Proposed pyrido[3,2-*d*]pyrmidine compounds.

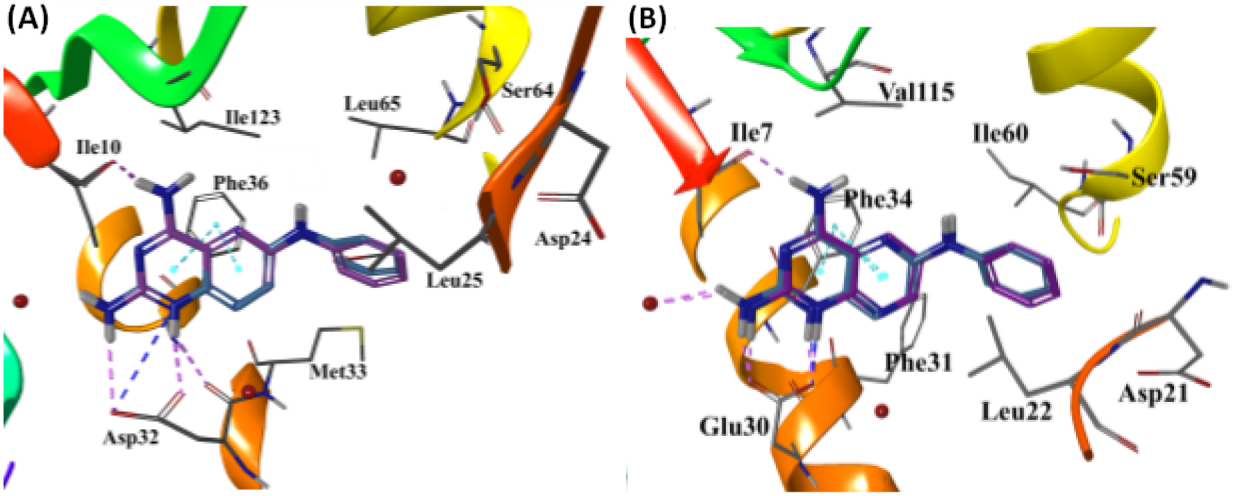

Figure 4. (A) Superimposition of docked pose of **1** (magenta) and **9** (cyan) in the homology model of pjDHFR and (B) Docked pose of **1** (magenta) and **9** (cyan) in the crystal structure of hDHFR (PDB: 4QJC, 1.62 Å)[30]

and the 2-NH_2 with Asp32. The 4-NH_2 moiety for both **9** and **18** forms hydrogen bonds with the backbone of Ile10 and the pyrrolo[3,2-*d*] pyrimidine scaffold is stabilized by π-π -stacking interaction with Phe36. The phenyl moiety is oriented in the pocket formed by Leu25, Met33, Ser64 and Leu65. The distance between Ile123 side chain and the N9- of the pyrido[3,2-*d*]pyrimidine **9** was 4.47 Å, whereas the distance between the Ile123 side chain and N9-methyl group of the pyrido [3,2-*d*]pyrimidine **18** was 3.43 Å. Since all other interactions are similar for **9** and **18**, the additional N^9-CH_3 on **18** can potentially have stronger hydrophobic interactions with pjDHFR, than **9**. The best docked poses for **9** and **18** in the pjDHFR homology model generated docking scores of −8.22 kcal/mol and −8.02 kcal/mol, respectively. Figure 5b displays the best docked conformation of **9** and **18** in hDHFR crystal structure (PDB: 4QJC, 1.61 Å).[30] The analogs exhibit a bidentate ionic interaction of the protonated N1 and 2-NH_2 with Glu30. The 4-NH_2 hydrogen bonds with the backbone of Ile7. The phenyl moiety is oriented in the pocket formed by Leu22, Phe31 and Ser59. The scaffold is stabilized by π-π-stacking interactions with Phe34. The distance between Val115 side chain and nitrogen substituted at the 6-position of the pyrido[3,2-*d*]pyrimidine **9** was 5.83 Å, whereas the distance between Val115 side chain and N^9-CH_3 of the pyrido[3,2-*d*]pyrimidine **18** as 4.36 Å. The best docked poses for **9** and **18** in hDHFR crystal structure generated docking scores of −8.87 kcal/mol and −9.39 kcal/mol, respectively. To further evaluate the optimum length of the alkyl moiety required to interact with Ile123 (in pjDHFR) and not the shorter Val115 (in hDHFR), longer and branched chain alkyl groups were designed for evaluation for substitution at the N^9-position. Thus, it was of interest to synthesize N^9-alkyl pyrido[3,2-*d*]pyrimidines **18–22**. All the proposed compounds **9–22** displayed better docking scores for pjDHFR over hDHFR, compared to the lead compound **1** (docking scores are included in the Supporting Information) indicating possible increase in potency and selectivity for pjDHFR over hDHFR.

Intermediate **25** (Scheme 1) was synthesized following a reported procedure.[35,36] The 2,6-dichloropyridine **23** was nitrated with 90% nitric acid and sulfuric acid, followed by substitution of the 2-Cl moiety with cuprous cyanide at 180 °C to afford 2-cyano-3-nitro-6-chloropyridine **25**. The structure of **25** was confirmed from the coupling constants (*J*) of the protons [^{1}H NMR (400 Hz) δ 7.80 (d, *J* = 7.2 Hz, 1H), 8.58 (d, *J* = 7.2 Hz, 1H)]. The coupling constants match the characteristic J constants for ortho coupling between aromatic protons.[37]

Following the reported procedure,[38] synthesis of **26** (Scheme 1) was attempted. Compound **25** was reacted with the 3,4,5-trifluoroaniline in monoethylglycol in the presence of pyridine at 140 °C. The reaction did not yield any product after 12 h. The reason for the failure of the reaction could be the poor nucleophilicity of the 3,4,5-trifluoroaniline.

In order to carry out the displacement with a weak nucleophile such as 3,4,5-trifluoroaniline on **25**, the alternate methodology reported by Gangjee *et al.*[38] was followed (Scheme 2). The 3,4,5-trifluoroaniline was first treated with LDA at −78 °C to afford a more reactive nitrogen

Table 3
Inhibition Concentrations (IC_{50}) of **9–22** against pjDHFR and hDHFR and Selectivity Ratios.

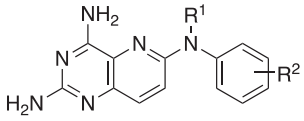

9-22

#	R^1	R^2	pjDHFR (IC_{50}, in nM)	hDHFR (IC_{50}, in nM)	Selectivity Ratio [hDHFR/ pjDHFR]
9	H	H	122	1526	13
10	H	4′-CH_3	174	2626	15
11	H	4′-OCH_3	239	2459	10
12	H	4′-OH	150	1576	10
13	H	2′,3′-$(CH)_4$	112	1098	10
14	H	3′,4′-$(CH)_4$	275	3185	12
15	H	3′,4′,5′-triF	80	2253	28
16	H	3′,4′-diF	155	1808	12
17	H	4′-OCF_3	194	4125	21
18	CH_3	H	96	942	10
29	CH_2CH_3	H	150	1571	10
20	$CH_2CH_2CH_3$	H	123	1338	11
21	$CH(CH_3)_2$	H	201	1373	7
22	$CH_2CH_2CH_2CH_3$	H	66	903	14
TMP[b]			92	24,500	266
PTX[c]			41	2	0.05

[a]These assays were carried out at 37 °C under 9 μM dihydrofolic acid concentration. The standard error of the means for these values is 12% or less than the mean value; [b]Trimethoprim; [c]Piritrexim.

anion, followed by displacement of the 6-chloro group of **25** to afford **26** in 10% yield.

The syntheses of **9–22** were accomplished from **25** as shown in Scheme 2. To a solution of 6-chloro-3-nitro-2-pyridinecarbonitrile (**25**) in isopropanol, the appropriate aniline was added and the mixture was heated at 130 °C (Scheme 1). After 3–16 h, the solution was concentrated under reduced pressure to afford **26–38.** This step using isopropanol afforded increased yields and provided safer conditions, compared to the displacement using LDA. The mixture was not separated and was advanced to the next step. The nitro compounds **26–38** were reduced using iron powder in concentrated hydrochloric acid to afford **39–52**.[38] The formation of the amino compounds **39–52** is indicated by a blue fluorescence on TLC at 254 nm. These amino compounds **39–52** were not separated and advanced to the cyclization step. During the reduction of **29** to **41** (R^2 = 4-OCH_3), the methoxy group undergoes partial ether cleavage in the work up step and afforded two very close spots on the TLC (possibly for **41** and **42**). To obtain the target compounds, the reported method[38] was followed for the cyclization of **39–52** in dimethyl sulfone at 140 °C to afford **9–22**.

Table 3 displays the IC_{50} values of compounds **9–22** for pjDHFR and hDHFR. Comparison of activities of pyrido[3,2-*d*]pyrimidines vs. pyrido[2,3-*d*]pyrimidines for pjDHFR, hDHFR and selectivity ratios, indicates that the scaffold replacement strategy was favorable. Biological evaluation of **9** against pjDHFR and hDHFR displayed an improvement of greater than 2-fold in pjDHFR potency, compared to its regio isomer **1** (Table 3).[28] Additionally, the selectivity for pjDHFR over hDHFR for **9** also improved significantly (> 13-fold), compared to **1.**

As observed for pyrido[3,2-*d*]pyrimidine **9**, a considerable improvement in selectivity was seen for compounds **10** (vs. **2**), **11** (vs. **3**), **13** (vs. **4**), **14** (vs. **5**), and **15** and **16** (vs. **6**), validating the rationale of the scaffold hopping strategy. The trifluoro-substituted analog **15** showed the highest selectivity for pjDHFR over hDHFR in the series, which is 560-fold greater than the selectivity ratio of PTX. Compared to its pyrido[2,3-*d*]pyrimidine analog **6**, **15** showed an 11-fold improvement in the potency towards pjDHFR and a 7-fold improvement in the selectivity ratio for pjDHFR over hDHFR. The improved potency and selectivity of **15** for pjDHFR could be due to a better binding of **15** with the active site of pjDHFR compared to that of other ligands.

The alkyl analogs **18–22** in the N^9-substituted pyrido[3,2-*d*]pyrimidine-2,4,6-triamines were designed to obtain better hydrophobic interactions with Ile123 (in pjDHFR) vs. Val115 (in hDHFR). The N^9-alkyl analogs **18–21** did not show a significant improvement in pjDHFR potency and selectivity, compared to the N^9-H analog **9**. The absence of improvement in potency and/or selectivity for pjDHFR could be due to the smaller size of the alkyl groups, which are not able to effectively interact with Ile123 in the pjDHFR active site. The N^9-butyl analog **22** demonstrated the best potency for pjDHFR of the series which could be attributed to the length of the butyl substitution which can interact with Ile123 (pjDHFR) better than the smaller alkyl groups of **18–21**. Compound **22** with the best potency (IC_{50}, 66 nM) against pjDHFR demonstrated a 14-fold selectivity for pjDHFR, whereas **15** despite a comparatively lower potency for pjDHFR (IC_{50}, 80 nM) showed a significantly higher selectivity. Thus, in the N^9-substituted pyrido[3,2-*d*]pyrimidine-2,4,6-triamine series, **15** remained the best in terms of its potency and selectivity for pjDHFR. Though the selectivities of some of these compounds fall short of that for TMP for pjDHFR, the potency is

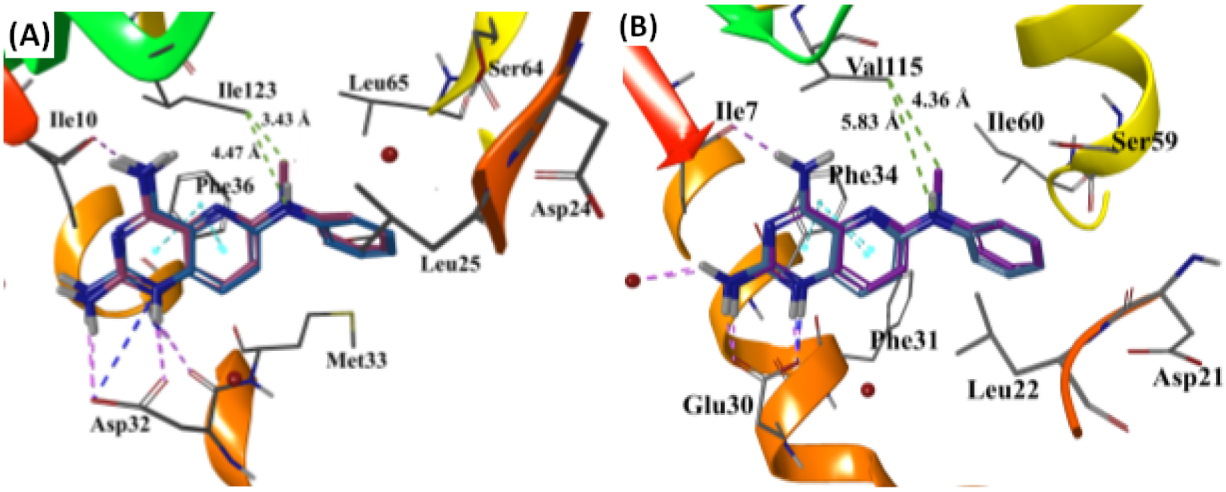

Figure 5. (A) Superimposition of docked pose of **9** (cyan) and **18** (magenta) in the homology model of pjDHFR and (B) Docked pose of **9** (cyan) and **18** (magenta) in the crystal structure of hDHFR (PDB: 4QJC, 1.62 Å)[30]

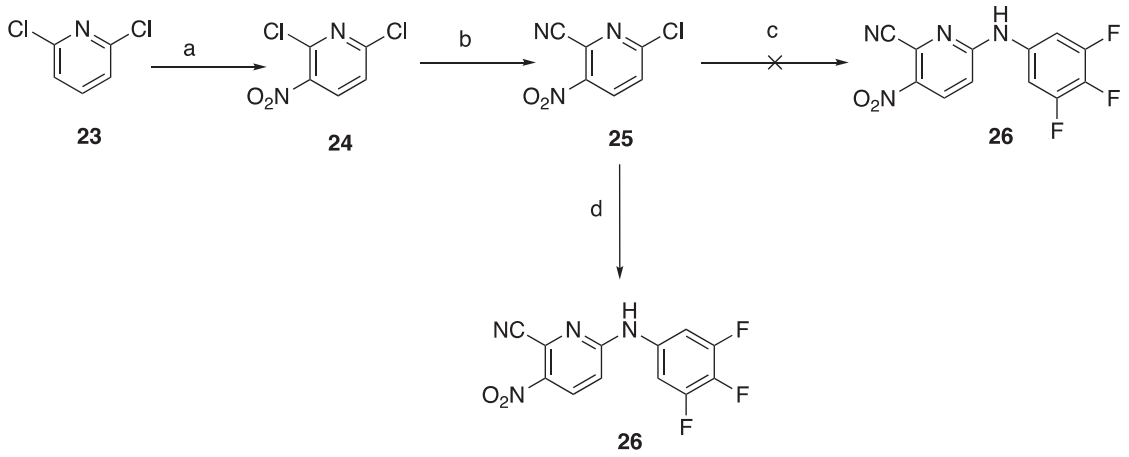

Scheme 1. Synthesis of intermediate **26.** a) 0% HNO_3, H_2SO_4, reflux, 3 h; b) CuCN, 180 °C, 15 min; c) aniline, monoethyl glycol, pyridine, 140 °C, 12 h; d) aniline, LDA, THF, −78 °C, 12 h.

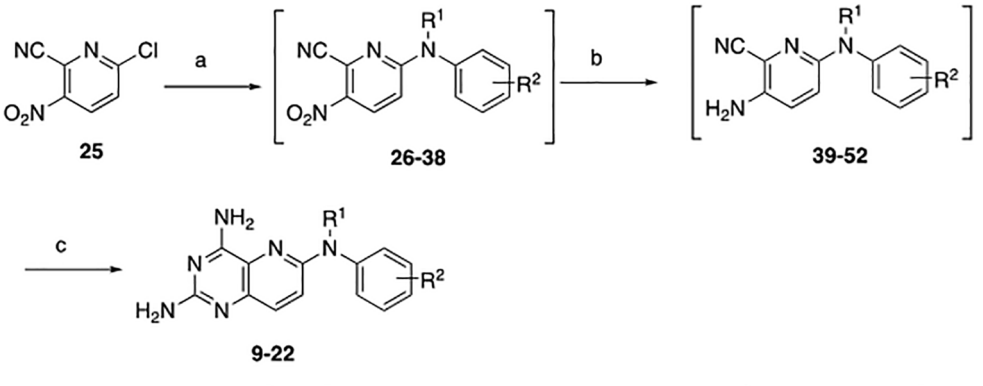

Scheme 2. Synthesis of target compounds **9–22.** a) substituted aniline, isopropanol, 130 °C, 3–16 h; b) conc. HCl, Fe powder, reflux, 0.5–2 h; c) chlorformamidine HCl, dimethyl sulfone, 140 °C, 3–16 h.

				R^1	R^2					R^1	R^2
27	**39**	**9**	(15%)	H	H	**33**	**47**	**17**	(15%)	H	4'-OCF_3
28	**40**	**10**	(14%)	H	4'-CH_3	**34**	**48**	**18**	(14%)	CH_3	H
29	**41**	**11**	(03%)	H	4'-OCH_3	**35**	**49**	**19**	(03%)	CH_2CH_3	H
29	**42**	**12**	(04%)	H	4'-OH	**36**	**50**	**20**	(04%)	$CH_2CH_2CH_3$	H
30	**43**	**13**	(12%)	H	2',3'-$(CH)_4$	**37**	**51**	**21**	(12%)	$CH(CH_3)_2$	H
31	**44**	**14**	(15%)	H	3',4'-$(CH)_4$	**38**	**52**	**22**	(15%)	$CH_2CH_2CH_2CH_3$	H
32	**45**	**15**	(21%)	H	3',4'-diF						
26	**46**	**16**	(16%)	H	3',4',5'-triF						

equivalent or slightly better than TMP. Utilizing the information provided by this study, the design and synthesis of potentially more potent and selective compounds are currently underway and will be the subject of future reports.

Acknowledgement

This work was supported, in part, by grants from the National Institute of Health (NIH), National Institute of Allergy and Infectious Diseases (NIAID), RO1AI098458, Adrian van Kaam Chair in Scholarly Excellence (AG) Duquesne University, and NSF for NMRs.

Appendix A. Supplementary data

Supplementary data to this article can be found online at https://doi.org/10.1016/j.bmcl.2019.06.004.

References

1. Sokulska M, Kicia M, Wesołowska M, Hendrich AB. Pneumocystis jirovecii—from a commensal to pathogen: clinical and diagnostic review. *Parasit Res.* 2015;114:3577–3585.
2. Yiannakis EP, Boswell TC. Systematic review of outbreaks of Pneumocystis jirovecii pneumonia: evidence that P. jirovecii is a transmissible organism and the implications for healthcare infection control. *J Hospital Infection.* 2016;93:1–8.
3. Truong J, Ashurst JV. Pneumonia, Pneumocystis (Carinii) Jiroveci. [Updated 2018 Feb 23]. In: StatPearls [Internet]. Treasure Island (FL): StatPearls Publishing; 2018 Jan-. Available from: https://www.ncbi.nlm.nih.gov/books/NBK482370/.
4. Chew LC, Maceda-Galang LM, Tan YK, Chakraborty B, Thumboo J. Pneumocystis jirovecii pneumonia in patients with autoimmune disease on high-dose glucocorticoid. *J Clin Rheumatol Practical Rep Rheumatic Musculoskeletal Dis.* 2015;21:72–75.
5. Guarner J. Human immunodeficiency virus and fungal infections. *Semin Diagn Pathol.* 2017;34:325–331.
6. Kostakis ID, Sotiropoulos GC, Kouraklis G. Pneumocystis jirovecii pneumonia in liver transplant recipients: a systematic review. *Transpl Proc.* 2014;46:3206–3208.
7. Lee KY, Ho CC, Ji DD, et al. Etiology of pulmonary complications of human immunodeficiency virus-1-infected patients in Taiwan in the era of combination antiretroviral therapy: a prospective observational study,. *J microbiol Immunol Infection = Wei mian yu gan ran za zhi.* 2013;46:433–440.
8. Buchacz K, Baker RK, Moorman AC, et al. Rates of hospitalizations and associated diagnoses in a large multisite cohort of HIV patients in the United States, 1994–2005. *AIDS (London, England).* 2008;22:1345–1354.
9. Smith CJ, Ryom L, Weber R, et al. to 2011 (D:A:D): a multicohort collaboration. *Lancet.* 1999;384(2014):241–248.
10. Neuhaus J, Angus B, Kowalska JD, et al. Risk of all-cause mortality associated with nonfatal AIDS and serious non-AIDS events among adults infected with HIV. *AIDS (London, England).* 2010;24:697–706.
11. Castro JG, Morrison-Bryant M. Management of Pneumocystis Jirovecii pneumonia in HIV infected patients: current options, challenges and future directions. *HIV/AIDS (Auckland, N.Z.).* 2010;2:123–134.

12. Harris JR, Balajee SA, Park BJ. Pneumocystis Jirovecii Pneumonia: Current Knowledge and Outstanding Public Health Issues. *Curr Fungal Infect Reports.* 2010;4:229–237.
13. Bernheimer JM, Patten G, Makeleni T, et al. Paediatric HIV treatment failure: a silent epidemic. *J Int AIDS Society.* 2015;18:20090.
14. Armstrong-James D, Meintjes G, Brown GD. A neglected epidemic: fungal infections in HIV/AIDS. *Trends Microbiol.* 2014;22:120–127.
15. Masur H, Brooks JT, Benson CA, Holmes KK, Pau AK, Kaplan JE. Prevention and treatment of opportunistic infections in HIV-infected adults and adolescents: Updated Guidelines from the Centers for Disease Control and Prevention, National Institutes of Health, and HIV Medicine Association of the Infectious Diseases Society of America. *Clinical infectious diseases : an official publication of the Infectious Diseases Society of America.* 2014;58:1308–1311.
16. Miller RF, Huang L, Walzer PD. Pneumocystis Pneumonia Associated with Human Immunodeficiency Virus. *Clin Chest Med.* 2013;34:229–241.
17. Hawser S, Lociuro S, Islam K. Dihydrofolate reductase inhibitors as antibacterial agents. *Biochem Pharmacol.* 2006;71:941–948.
18. Yoon C, Subramanian A, Chi A, et al. Dihydropteroate Synthase Mutations in Pneumocystis Pneumonia: Impact of Applying Different Definitions of Prophylaxis, Mortality Endpoints and Mutant in a Single Cohort. *Med Mycol.* 2013;51:568–575.
19. Gordin FM, Simon GL, Wofsy CB, Mills J. ADverse reactions to trimethoprim-sulfamethoxazole in patients with the acquired immunodeficiency syndrome. *Ann Intern Med.* 1984;100:495–499.
20. Temesgen Z, Beri G. HIV and drug allergy. *Immunol Allergy Clin N Am.* 2004;24:521–531 viii.
21. Sangiolo D, Storer B, Nash R, et al. Toxicity and Efficacy of Daily Dapsone as Pneumocystis jiroveci Prophylaxis after Hematopoietic Stem Cell Transplantation: A Case-Control Study. *Biol Blood Marrow Transplant.* 2005;11:521–529.
22. White NJ. Cardiotoxicity of antimalarial drugs. *Lancet Infect Dis.* 2007;7:549–558.
23. Nickel P, Schurmann M, Albrecht H, et al. Clindamycin-primaquine for pneumocystis jiroveci pneumonia in renal transplant patients. *Infection.* 2014;42:981–989.
24. Wharton JM, Coleman DL, Wofsy CB, et al. Trimethoprim-sulfamethoxazole or pentamidine for Pneumocystis carinii pneumonia in the acquired immunodeficiency syndrome A prospective randomized trial. *Ann Intern Med.* 1986;105:37–44.
25. Kovacs JA, Allegra CJ, Swan JC, et al. Potent antipneumocystis and antitoxoplasma activities of piritrexim, a lipid-soluble antifolate. *Antimicrob Agents Chemother.* 1988;32:430–433.
26. Short C-ES, Gilleece YC, Fisher MJ, Churchill DR. Trimetrexate and folinic acid: a valuable salvage option for Pneumocystis jirovecii pneumonia. *AIDS.* 2009;23:1287–1290.
27. Wakefield AE. Genetic heterogeneity in Pneumocystis carinii: an introduction. *FEMS Immunol Med Microbiol.* 1998;22:5–13.
28. Gangjee A, Namjoshi OA, Raghavan S, Queener SF, Kisliuk RL, Cody V. Design, synthesis, and molecular modeling of novel pyrido[2,3-*d*]pyrimidine analogues as antifolates; application of Buchwald-Hartwig aminations of heterocycles. *J Med Chem.* 2013;56:4422–4441.
29. Cody V, Chisum K, Pope C, Queener SF. Purification and characterization of human-derived Pneumocystis jirovecii dihydrofolate reductase expressed in Sf21 insect cells and in Escherichia coli. *Protein Expr Purif.* 2005;40:417–423.
30. Cody V, Pace J, Namjoshi OA, Gangjee A. Structure-activity correlations for three pyrido[2,3-*d*]pyrimidine antifolates binding to human and Pneumocystis carinii dihydrofolate reductase. *Acta Crystallogr. F Struct. Biol. Commun.* 2015;71:799–803.
31. Small-Molecule Drug Discovery Suite 2018-2, Schrödinger, LLC, New York, NY, 2018.
32. Shah K, Lin X, Queener SF, Cody V, Pace J, Gangjee A. Targeting species specific amino acid residues: Design, synthesis and biological evaluation of 6-substituted pyrrolo[2,3-d]pyrimidines as dihydrofolate reductase inhibitors and potential anti-opportunistic infection agents. *Bioorg Med Chem.* 2018;26:2640–2650.
33. Rosowsky A, Forsch RA, Queener SF. 2,4-Diaminopyrido[3,2-d]pyrimidine Inhibitors of Dihydrofolate Reductase from Pneumocystis carinii and Toxoplasma gondii. *J Med Chem.* 1995;38:2615–2620.
34. Gangjee A, Adair OO, Queener SF. Synthesis and Biological Evaluation of 2,4-Diamino-6-(arylaminomethyl)pyrido[2,3-d]pyrimidines as Inhibitors of Pneumocystis carinii and Toxoplasma gondii Dihydrofolate Reductase and as Antiopportunistic Infection and Antitumor Agents. *J Med Chem.* 2003;46:5074–5082.
35. Colbry NL, Elslager EF, Werbel LM. Synthesis and antimalarial properties of 2,4-diamino-6-[(aryl)thio, sulfinyl, and sulfonyl]pyrido[3,2-d]pyrimidines. *J Heterocycl Chem.* 1984;21:1521–1525.
36. Colbry NL, Elslager EF, Werbel LM. Folate antagonists. 21. Synthesis and antimalarial properties of 2,4-diamino-6-(benzylamino)pyrido[3,2-*d*]pyrimidines. *J Med Chem.* 1985;28:248–252.
37. Silverstein RM, Webster FX, Kiemle D. *Spectrometric Identification of Organic Compounds.* 7th Edition Wiley; 2005.
38. Gangjee A, Zhu Y, Queener SF. 6-Substituted 2,4-Diaminopyrido[3,2-*d*]pyrimidine Analogues of Piritrexim as Inhibitors of Dihydrofolate Reductase from Rat Liver, Pneumocystis carinii, and Toxoplasma gondii and as Antitumor Agents. *J Med Chem.* 1998;41:4533–4541.